

# PARTICLE SWARM OPTIMISATION AIDED MULTIUSER TRANSMISSION SCHEMES FOR MIMO COMMUNICATION

Wang Yao, Sheng Chen, Lajos Hanzo

*School of Electronics and Computer Science, University of Southampton, Southampton SO17 1BJ, UK  
wy07r@ecs.soton.ac.uk, sqc@ecs.soton.ac.uk, lh@ecs.soton.ac.uk*

**Keywords:** Bio-inspired computation, evolutionary computation, particle swarm optimisation, multiple-input multiple-output communication, multiuser transmission, precoding, vector precoding.

**Abstract:** Bio-inspired computational methods have found wide-ranging applications in signal processing and other walks of engineering. In this contribution, particle swarm optimisation (PSO) is invoked for designing optimal multiuser transmission (MUT) schemes for multiple-input multiple-output communication. Specifically, we consider the minimum bit-error-rate (MBER) linear MUT using PSO and we design a PSO aided MBER generalised vector precoding for nonlinear MUT. These PSO aided MUT techniques compare favourably with the state-of-the-art conventional schemes, in terms of performance and complexity.

## 1 Introduction

Bio-inspired computational methods have found ever-increasing applications in all walks of engineering, especially communication signal processing, where attaining global or near global optimal solutions at affordable computational costs are critical. Genetic algorithms and ant colony optimisation have been adopted in communication applications (Chen et al., 1997; Chen and Wu, 1998; Yen, 2001; Alias et al., 2005; Xu et al., 2008a; Xu et al., 2008b). Recently, particle swarm optimisation (PSO) (Kennedy and Eberhart, 1995) has become popular and has been applied to a variety of applications (Kennedy and Eberhart, 2001; Ratnaweera et al., 2004; Guru et al., 2005; Feng, 2006; Soo et al., 2007). PSO constitutes a population based stochastic optimisation technique, inspired by the social behaviour of bird flocks or fish schools. The algorithm commences with random initialisation of a swarm of individuals, referred to as particles, within the problem's search space. Each particle then gradually adjusts its trajectory with the aid of cognitive information (its own best location) and social information (the best position of the entire swarm) at each evolutionary step. PSO is simple to implement, has ability to rapidly converge and is capable of steering clear of local minima.

This contribution designs optimal multiuser transmission (MUT) schemes for multiple-input multiple-output (MIMO) communication systems with the aid of PSO. In the downlink of the MIMO system, the base station (BS), equipped with multiple transmit

antennas, communicates with single-receive-antenna mobile stations (MSs). Simple low-complexity MSs are incapable of performing sophisticated cooperative multiuser detection to mitigating the multiuser interference. A solution is to pre-process the transmitted multiuser downlink signals at the BS, leading to appealing MUT, provided that the BS has the knowledge of the downlink channel matrix. MUT schemes can be divided into the two groups, namely, linear MUT schemes and nonlinear MUT schemes.

A well-known linear MUT design is based on the minimum mean square error criterion (Vojčić and Jang, 1998), which has appealing simplicity but is limited by its achievable bit error rate (BER) performance. The optimal linear MUT design has been developed based on the minimum BER (MBER) criterion (Habendorf and Fettweis, 2007). The linear MBER-MUT design invokes a constrained nonlinear optimisation and the sequential quadratic programming (SQP) algorithm (Nocedal and Wright, 1999) is typically used to obtain the precoder's coefficients. However, the computational complexity of the SQP based MBER-MUT solution can be excessive for high-rate systems. In this contribution, we invoke the PSO to solve the constrained nonlinear optimisation problem for the MBER-MUT, and we show that the PSO aided MBER-MUT scheme provides improved performance in comparison to the conventional MMSE-MUT scheme, while imposing a significantly reduced complexity compared to the state-of-the-art SQP based MBER-MUT design.

A powerful nonlinear MUT technique known as

vector precoding (VP) is capable of significantly outperforming any linear MUT technique, particularly in the rank-deficient scenario where the number of the BS transmit antennas is smaller than the number of MSs supported. In the VP precoder, the data vector is perturbed by a perturbation vector, which is then multiplied by the precoding matrix to generate the effective symbol vector to be transmitted. The design is then to determine the precoding matrix and the perturbation vector separately. The existing powerful VP design is the nonlinear MMSE VP scheme (Schmidt et al., 2005). We propose to generate the effective symbol vector directly by minimising the BER criterion. This generalised MBER VP design is a challenging non-convex optimisation, and we adopt the efficient PSO algorithm to solve this design. The proposed PSO aided generalised MBER VP is shown to dramatically outperform the existing powerful nonlinear MMSE VP benchmark (Schmidt et al., 2005), at a cost of slightly increased computational complexity.

The following notational conventions are adopted in this contribution. Boldface capitals and lower-case letters stand for matrices and vectors, respectively. Furthermore,  $()^T$  represents the transpose operator, while  $\|\cdot\|^2$  and  $\|\cdot\|$  denote the norm and the magnitude operators, respectively.  $E[\cdot]$  denotes the expectation operator, while  $\Re[\cdot]$  and  $\Im[\cdot]$  represent the real and imaginary parts, respectively. Finally,  $j = \sqrt{-1}$ .

## 2 Particle Swarm Optimisation

Consider the optimisation task defined as follows

$$\mathbf{U}_{\text{opt}} = \arg \min_{\mathbf{U}} F(\mathbf{U}) \quad (1)$$

$$\text{s.t. } \mathbf{U} \in \mathcal{U}^{N \times M} \quad (2)$$

where  $F(\cdot)$  is the cost function,  $\mathbf{U}$  is a  $N \times M$  complex-valued parameter matrix to be optimised, and

$$\mathcal{U} = [-U_{\max}, U_{\max}] + j[-U_{\max}, U_{\max}] \quad (3)$$

defines the search range for each element of  $\mathbf{U}$ . The flowchart of the PSO algorithm is given in Fig. 1. A swarm of particles,  $\{\mathbf{U}_i^{(l)}\}_{i=1}^S$ , that represent potential solutions are evolved in the search space  $\mathcal{U}^{N \times M}$ , where  $S$  is the swarm size and index  $l$  denotes the iteration step. The algorithm is now summarised.

### 2.1 PSO algorithm

*a) Initialisation.* Set  $l = 0$  and randomly generate the initial particles,  $\{\mathbf{U}_i^{(l)}\}_{i=1}^S$ , in the search space  $\mathcal{U}^{N \times M}$ .

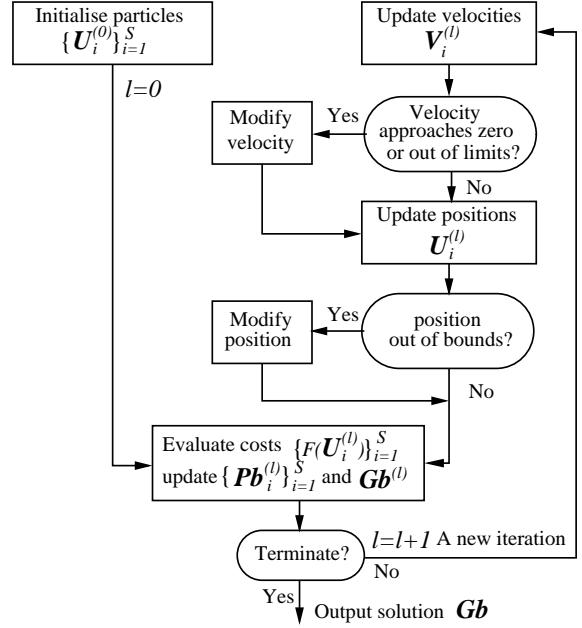


Figure 1: Flowchart of the PSO algorithm.

*b) Evaluation.* Each particle  $\mathbf{U}_i^{(l)}$  has an associated cost  $F(\mathbf{U}_i^{(l)})$ , and it remembers its best position visited so far, denoted as  $\mathbf{Pb}_i^{(l)}$ , which provides the cognitive information. Every particle also knows the best position visited so far among the entire swarm, denoted as  $\mathbf{Gb}^{(l)}$ , which provides the social information. The cognitive information  $\{\mathbf{Pb}_i^{(l)}\}_{i=1}^S$  and the social information  $\mathbf{Gb}^{(l)}$  are updated at each iteration given the new cost information  $\{F(\mathbf{U}_i^{(l)})\}_{i=1}^S$ .

*c) Update.* Each particle  $\mathbf{U}_i^{(l)}$  has a velocity, denoted as  $\mathbf{V}_i^{(l)}$ , to direct its “flying” or search. The velocity and position of the  $i$ th particle are updated in each iteration according to:

$$\begin{aligned} \mathbf{V}_i^{(l+1)} = & \xi * \mathbf{V}_i^{(l)} + c_1 * \phi_1 * (\mathbf{Pb}_i^{(l)} - \mathbf{U}_i^{(l)}) \\ & + c_2 * \phi_2 * (\mathbf{Gb}^{(l)} - \mathbf{U}_i^{(l)}), \end{aligned} \quad (4)$$

$$\mathbf{U}_i^{(l+1)} = \mathbf{U}_i^{(l)} + \mathbf{V}_i^{(l+1)}, \quad (5)$$

where  $\xi$  is the inertia weight,  $c_1$  and  $c_2$  are the two acceleration coefficients, while  $\phi_1 = \text{rand}()$  and  $\phi_2 = \text{rand}()$  denotes the two random variables uniformly distributed in  $(0, 1)$ .

In order to avoid excessive roaming of particles beyond the search space, a velocity space  $\mathcal{V}^{N \times M}$  with

$$\mathcal{V} = [-V_{\max}, V_{\max}] + j[-V_{\max}, V_{\max}] \quad (6)$$

is imposed so that each element of  $\mathbf{V}_i^{(l+1)}$  is within the search range  $\mathcal{V}$  defined in (6). Furthermore, if an element of  $\mathbf{V}_i^{(l+1)}$  approaches zero, it may be randomly

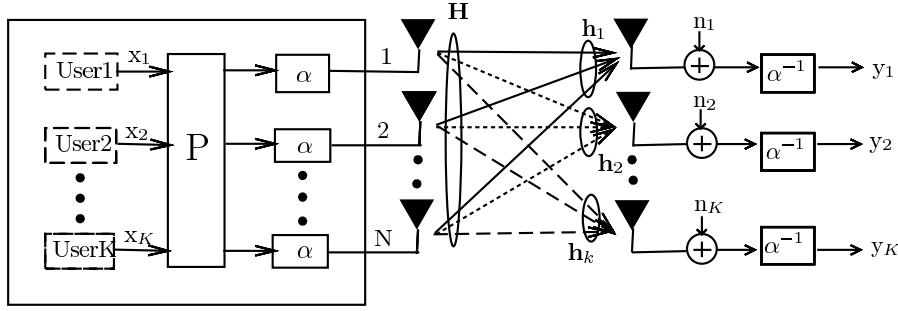


Figure 2: MUT-aided MIMO system with linear precoding, where the BS employs  $N$  transmit antennas to communicate with  $K$  single-antenna mobile devices.

reinitialised within the velocity range  $V$ . Similarly, if a particle  $\mathbf{U}_i^{(l+1)}$  moves to outside the search space, it is moved back inside  $\mathcal{U}^{N \times M}$  randomly.

*d) Termination.* If the maximum number of iterations,  $I_{\max}$ , is reached, terminate with the solution  $\mathbf{U}_{\text{opt}} = \mathbf{G}\mathbf{b}^{(I_{\max})}$ ; otherwise, set  $l = l + 1$  and go to Step *b*).

## 2.2 PSO algorithmic parameters

The search limit  $U_{\max}$  is specified by the problem considered, while the velocity limit  $V_{\max}$  is typically related to  $U_{\max}$ . Three common choices of the inertia weight are  $\xi = 0$ , setting  $\xi$  to a small positive constant, and  $\xi = \text{rand}()$ . The time varying acceleration coefficients (Ratnaweera et al., 2004), in which  $c_1$  is reduced from 2.5 to 0.5 and  $c_2$  varies from 0.5 to 2.5 during the iterative procedure according to

$$\begin{aligned} c_1 &= (0.5 - 2.5) * l / I_{\max} + 2.5, \\ c_2 &= (2.5 - 0.5) * l / I_{\max} + 0.5, \end{aligned} \quad (7)$$

usually works well. Appropriate values for  $S$  and  $I_{\max}$  can be chosen to ensure that the algorithm converges to the optimal solution with a minimum computational complexity.

Let the complexity of one cost function evaluation be  $C_{\text{single}}$ . With the swarm size  $S$  and assuming that the algorithm converges in  $I_{\max}$  iterations, the number of cost function evaluations is  $N_{\text{total}} = S \times I_{\max}$ , and the complexity of the algorithm is given by

$$C_{\text{PSO}} = N_{\text{total}} \times C_{\text{single}} = S \times I_{\max} \times C_{\text{single}}. \quad (8)$$

## 3 Linear MBER MUT Design

Our first application involves the PSO aided linear MBER MUT design.

### 3.1 Linear MUT system model

The linear MUT-aided MIMO system is depicted in Fig. 2, where the BS equipped with  $N$  transmit an-

tennas communicates with  $K$  MSs, each employing a single-antenna. The information symbol vector transmitted is given by  $\mathbf{x} = [x_1 \ x_2 \ \dots \ x_K]^T$ , where  $x_k$  denotes the transmitted symbol to the  $k$ th MS and it takes the value from the 4-QAM symbol set

$$S = \left\{ \pm \frac{1}{2} \pm j \frac{1}{2} \right\}. \quad (9)$$

The MUT's  $N \times K$  precoder matrix  $\mathbf{P}$  is defined by

$$\mathbf{P} = [\mathbf{p}_1 \ \mathbf{p}_2 \ \dots \ \mathbf{p}_K], \quad (10)$$

where  $\mathbf{p}_k$ ,  $1 \leq k \leq K$ , is the precoder's coefficient vector for the  $k$ th user's data stream. Given a fixed total transmit power  $E_T$  at the BS, an appropriate scaling factor should be used to fulfill this transmit power constraint, which is defined as  $\alpha = \sqrt{E_T / \|\mathbf{P}\mathbf{x}\|^2}$ .

At the receiver, the reciprocal of  $\alpha$  is used to scale the received signal to ensure unity-gain transmission. The MIMO channel matrix  $\mathbf{H}$  is given by

$$\mathbf{H} = [\mathbf{h}_1 \ \mathbf{h}_2 \ \dots \ \mathbf{h}_K], \quad (11)$$

where  $\mathbf{h}_k = [h_{1,k} \ h_{2,k} \ \dots \ h_{N,k}]^T$ ,  $1 \leq k \leq K$ , is the  $k$ th user's spatial signature. The channel taps  $h_{i,k}$  for  $1 \leq k \leq K$  and  $1 \leq i \leq N$  are independent of each other and obey the complex-valued Gaussian distribution with  $E[|h_{i,k}|^2] = 1$ . The additive white Gaussian noise vector  $\mathbf{n}$  is defined by  $\mathbf{n} = [n_1 \ n_2 \ \dots \ n_K]^T$ , where  $n_k$ ,  $1 \leq k \leq K$ , is a complex-valued Gaussian white noise with  $E[|n_k|^2] = 2\sigma_n^2 = N_0$ . The signal-to-noise ratio (SNR) of the system is defined as  $\text{SNR} = E_b / N_0$ , where  $E_b = E_T / (N \log_2 \mathcal{M})$  is the energy per bit per antenna for  $\mathcal{M}$ -ary modulation. For the 4-QAM case  $\mathcal{M} = 4$ . The system model is given by

$$\mathbf{y} = \mathbf{H}^T \mathbf{P}\mathbf{x} + \alpha^{-1} \mathbf{n}, \quad (12)$$

where  $\mathbf{y} = [y_1 \ y_2 \ \dots \ y_K]^T$  denotes the received signal vector, and  $y_k$ ,  $1 \leq k \leq K$ , constitutes sufficient statistics for the  $k$ th MS to detect the transmitted data symbol  $x_k$ . Thus, the  $k$ th MS equipped with a conventional matched filter can simply estimate  $x_k$  by quantising  $y_k$ .

### 3.2 Linear MBER MUT design

Given the 4-QAM symbol vector  $\mathbf{x}$ , the average BER of the in-phase component of  $\mathbf{y}$  at the receivers is (Habendorf and Fettweis, 2007)

$$P_{e_I, \mathbf{x}} = \frac{1}{K} \sum_{k=1}^K Q \left( \frac{\text{sgn}(\Re[x_k]) \Re[\mathbf{h}_k^T \mathbf{P} \mathbf{x}]}{\sigma_n} \right), \quad (13)$$

where  $Q(\bullet)$  is the standard Gaussian error function. Similarly, given the symbol vector  $\mathbf{x}$ , the average BER of the quadrature-phase component of  $\mathbf{y}$  is

$$P_{e_Q, \mathbf{x}} = \frac{1}{K} \sum_{k=1}^K Q \left( \frac{\text{sgn}(\Im[x_k]) \Im[\mathbf{h}_k^T \mathbf{P} \mathbf{x}]}{\sigma_n} \right). \quad (14)$$

Thus, the resultant BER for the specific 4-QAM symbol  $\mathbf{x}$  is

$$P_{e, \mathbf{x}}(\mathbf{P}) = (P_{e_I, \mathbf{x}}(\mathbf{P}) + P_{e_Q, \mathbf{x}}(\mathbf{P}))/2. \quad (15)$$

Therefore, the MBER-MUT design is defined as the solution of the following constrained optimisation

$$\begin{aligned} \mathbf{P}_{\text{MBER}, \mathbf{x}} &= \arg \min_{\mathbf{P}} P_{e, \mathbf{x}}(\mathbf{P}) \\ \text{s.t. } &\|\mathbf{P} \mathbf{x}\|^2 = E_T. \end{aligned} \quad (16)$$

This constrained nonlinear optimisation is typically solved by an iterative gradient based algorithm known as the SQP (Habendorf and Fettweis, 2007). The SQP based design however has a high computational complexity. A PSO-aided design (Yao et al., 2009b) offers an attractive low-complexity alternative.

A penalty function approach is adopted to convert the constrained optimisation (16) into an unconstrained one which automatically meets the transmit power constraint. First define the cost function

$$F(\mathbf{P}) = P_{e, \mathbf{x}}(\mathbf{P}) + G_{\mathbf{x}}(\mathbf{P}) \quad (17)$$

with the penalty function given by

$$G_{\mathbf{x}}(\mathbf{P}) = \begin{cases} 0, & \|\mathbf{P} \mathbf{x}\|^2 - E_T \leq 0 \\ \lambda(\|\mathbf{P} \mathbf{x}\|^2 - E_T), & \|\mathbf{P} \mathbf{x}\|^2 - E_T > 0 \end{cases} \quad (18)$$

where the penalty factor  $\lambda > 0$  should be chosen appropriately so that the MBER-MUT design (16) becomes the following unconstrained optimisation

$$\mathbf{P}_{\text{MBER}, \mathbf{x}} = \arg \min_{\mathbf{P}} F(\mathbf{P}), \quad (19)$$

where the precoding matrix  $\mathbf{P} \in \mathbb{U}^{N \times K}$ . The PSO algorithm described in Section 2 can readily be adopted to solve this optimisation problem. For the system introduced in Subsection 3.1, our empirical results suggest that the search limit can be set to  $U_{\max} = 1$  while the velocity limit can be set to  $V_{\max} = 1$ . We also remove the influence of the previous velocity by setting  $\xi = 0$ , which works well for this application. In Step *a*), one of the initial particles is set to the MMSE-MUT solution (Habendorf and Fettweis, 2007).

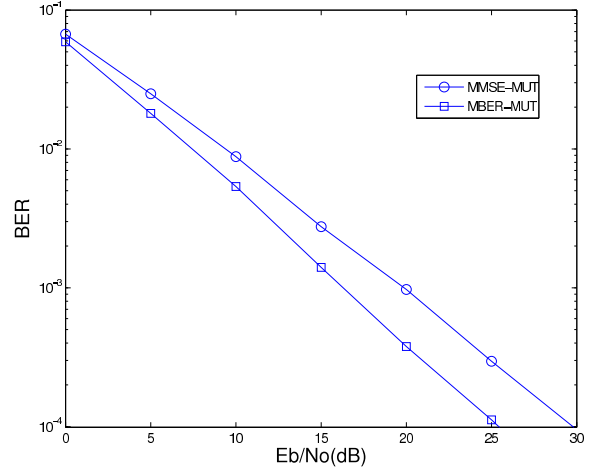


Figure 3: BER performance of the PSO-aided linear MBER-MUT design for the  $4 \times 4$  MIMO system, in comparison with the benchmark MMSE-MUT.

### 3.3 Simulation results

The MIMO system considered employed  $N = 4$  transmit antennas at the BS to communicate with  $K = 4$  MSs. All the simulation results were obtained by averaging over 100 channel realisations. An appropriate swarm size was found to be  $S = 20$  empirically. The maximum number of iterations,  $I_{\max}$ , was so chosen such that the PSO-based linear MBER-MUT algorithm with the chosen  $I_{\max}$  and  $S = 20$  arrived at the same MBER performance also achieved by the SQP-based MBER-MUT design. The value of  $I_{\max}$  was in the range of 20 to 30, depending on the value of the channel SNR. Fig. 3 compares the BER performance of the linear MMSE-MUT scheme with those

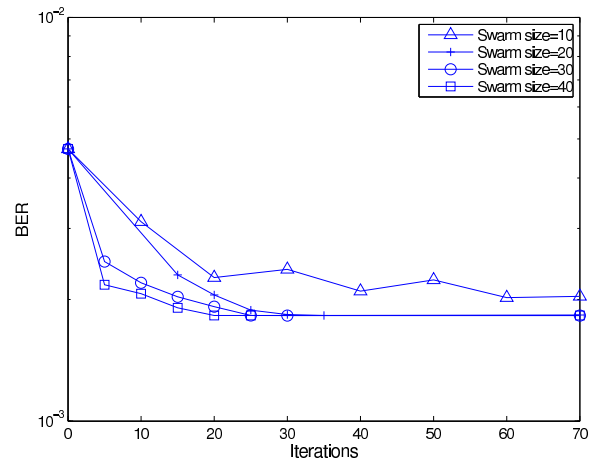


Figure 4: Convergence of the PSO MBER-MUT scheme with different swarm sizes for the  $4 \times 4$  MIMO system given SNR= 15 dB.

Table 1: Complexity (Flops) of the PSO aided linear MBER-MUT design with different swarm sizes for the  $4 \times 4$  MIMO system given SNR= 15 dB.

Swarm size $S$	20	30	40
Iterations $I_{\max}$	30	25	20
$C_{\text{PSO}}$ (Flops)	402,840	503,450	536,960

of the PSO-aided linear MBER-MUT design, where it can be seen that the PSO-aided MBER-MUT design achieved an SNR gain of 4.5 dB over the MMSE-MUT benchmark at the target BER of  $10^{-4}$ .

Given SNR= 15 dB, convergence performance of the PSO-aided linear MBER-MUT scheme with different swarm sizes are plotted in Fig. 4. It is clear from Fig. 4 that  $S = 10$  was insufficient for the PSO to attain the optimal solution, while the PSO algorithm with  $S = 20, 30$  and  $40$  all converged to the optimal solution after  $I_{\max} = 30, 25$  and  $20$ , respectively. The complexity  $C_{\text{PSO}}$  of the PSO-aided linear MBER-MUT scheme for these three values of  $S$  are listed in Table 1. We can see that the choice of  $S = 20$  was optimal for this case, in terms of complexity.

Computational complexity of the PSO-aided linear MBER-MUT scheme was then compared with that of the SQP-based one. Fig. 5 compares the convergence performance of the SQP and PSO based schemes, operating at the SNR values of 10 dB and 15 dB, respectively. It can be seen from Fig. 5 that in the case of SNR= 10 dB, the SQP and PSO algorithms converged to the optimal solution after 70 and 20 iterations, respectively, while at SNR= 15 dB, the SQP and PSO algorithms arrived at the optimal solution after 80 and 30 iterations, respectively. The complexity and recorded run times for the two designs are listed in Table 2. It can be seen from Table 2 that

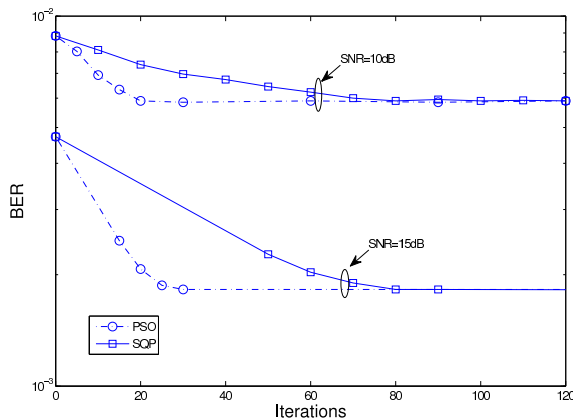


Figure 5: Convergence performance comparison of the PSO-aided and SQP-based MBER-MUT schemes for the  $4 \times 4$  MIMO system given two SNR values.

Table 2: Complexity (Flops) and recorded run time (s) comparison of the PSO and SQP aided linear MBER-MUT designs for the  $4 \times 4$  MIMO system given two SNR values.

(SNR= 10 dB)	SQP	PSO
Iterations	70	20
Complexity (Flops)	3,180,170	268,560
Run time (s)	7412.1	664.9
(SNR= 15 dB)	SQP	PSO
Iterations	80	30
Complexity (Flops)	3,634,480	402,840
Run time (s)	8457.3	957.4

the PSO-aided linear MBER-MUT design imposed an approximately twelve times lower complexity than the SQP counterpart at SNR= 10 dB, while it imposed an approximately nine times lower complexity than the SQP counterpart for the SNR value of 15 dB.

## 4 Nonlinear MBER MUT Design

Our second application considers the PSO aided nonlinear MBER generalised VP design.

### 4.1 Generic VP system model

The nonlinear MUT-aided MIMO system is depicted in Fig. 6, where the BS employs  $N$  transmit antennas to communicate with  $K$  single-antenna MS receivers each employing a modulo device. The channel matrix  $\mathbf{H}$ , the information symbol vector  $\mathbf{x}$ , and the noise vector  $\mathbf{n}$  are as defined in Subsection 3.1. Given  $\mathbf{x}$  and  $\mathbf{H}$ , the generic VP generates the continuous-valued effective symbol vector  $\mathbf{d} = [d_1 d_2 \dots d_N]^T$ , in order to mitigate multiuser interference. In a conventional VP design,  $\mathbf{d}$  is expressed as

$$\mathbf{d} = \mathbf{P}(\mathbf{x} + \boldsymbol{\omega}), \quad (20)$$

where  $\mathbf{P}$  is the  $N \times K$  precoding matrix and  $\boldsymbol{\omega}$  the  $K$ -element discrete-valued perturbation vector. The powerful MMSE VP scheme (Schmidt et al., 2005) determines the MMSE solution for  $\mathbf{P}$  and seeks  $\boldsymbol{\omega}$  based on the MMSE criterion. Our proposed generalised VP scheme, however, does not determine  $\mathbf{P}$  and  $\boldsymbol{\omega}$ . Rather it directly determines  $\mathbf{d}$ .

Given a fixed total transmit power  $E_T$  at the BS, an appropriate scaling factor,  $\alpha = \sqrt{E_T / \|\mathbf{d}\|^2}$ , is used to fulfill this transmit power constraint. At the receiver, the reciprocal of  $\alpha$  is used to scale the received signal in order to maintain a unity-gain transmission. The received signal vector  $\hat{\mathbf{y}} = [\hat{y}_1 \hat{y}_2 \dots \hat{y}_K]^T$  before the modulo operation is given by

$$\hat{\mathbf{y}} = \mathbf{H}^T \mathbf{d} + \alpha^{-1} \mathbf{n}. \quad (21)$$

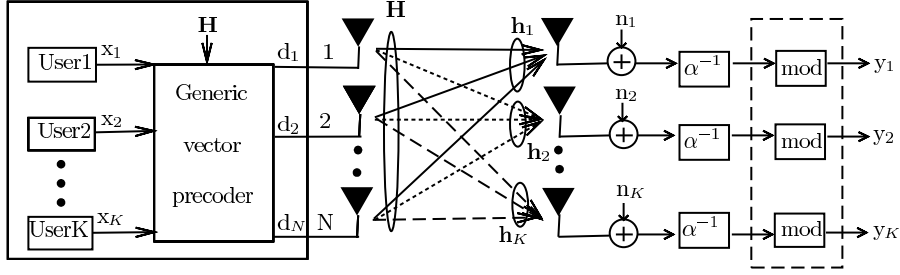


Figure 6: MUT-aided MIMO system with nonlinear VP, where the BS employs  $N$  transmit antennas to communicate with  $K$  MSs each equipped with a modulo device.

The modulo operation invoked for  $\hat{y}_k$  is described by

$$\text{mod}_\tau(\hat{y}_k) = \hat{y}_k - \lfloor \frac{\Re[\hat{y}_k] + \frac{\tau}{2}}{\tau} \rfloor \tau - j \lfloor \frac{\Im[\hat{y}_k] + \frac{\tau}{2}}{\tau} \rfloor \tau, \quad (22)$$

where  $\lfloor \bullet \rfloor$  denotes the integer floor operator, and  $\tau$  is a positive number determined by the modulation scheme. The received signal vector  $\mathbf{y} = [y_1 \ y_2 \ \dots \ y_K]^T$  after the modulo operation is given by

$$\mathbf{y} = \text{mod}_\tau(\hat{\mathbf{y}}), \quad (23)$$

and  $y_k$ ,  $1 \leq k \leq K$ , constitutes sufficient statistics for the  $k$ th MS to detect the transmitted information data symbol  $x_k$ . The work (Hochwald et al., 2005) suggested to choose  $\tau$  according to

$$\tau = 2(|c|_{\max} + \Delta/2), \quad (24)$$

where  $|c|_{\max}$  is the largest distance of the modulated symbols to the real or imaginary axis, and  $\Delta$  is the spacing between the constellation points. For the 4-QAM constellation (9),  $|c|_{\max} = \frac{1}{2}$  and  $\Delta = 1$ , which leads to  $\tau = 2$  according to (24). The modulo operator (22) maps the received signal,  $\Re[\hat{y}_k]$  and  $\Im[\hat{y}_k]$ , into the interval  $[-\tau/2, \tau/2)$ .

## 4.2 MBER generalised VP design

The BER encountered at the output of the receiver after the modulo operation for the in-phase component

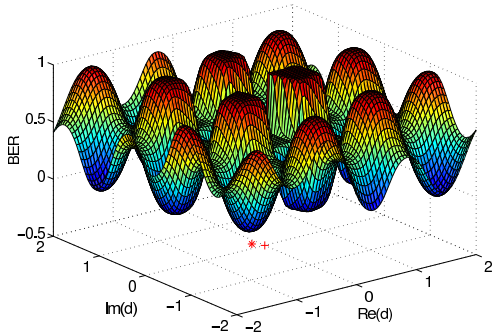


Figure 7: BER surface as a function of the effective symbol vector  $\mathbf{d}$  for the 4-QAM system with  $N = 1$  and  $K = 1$ , given SNR= 16 dB. The mark \* is the MBER generalised VP solution while the mark + is the MMSE VP solution.

of user  $k$  can be expressed as (Yao et al., 2010)

$$\begin{aligned} P_{eI,k}(\mathbf{d}) &\approx Q\left(\frac{c_R^{(k)} + 3\tau}{\alpha^{-1}\sigma_n}\right) + Q\left(\frac{-\frac{5\tau}{2} - c_R^{(k)}}{\alpha^{-1}\sigma_n}\right) \\ &- Q\left(\frac{-2\tau - c_R^{(k)}}{\alpha^{-1}\sigma_n}\right) + Q\left(\frac{-\frac{3\tau}{2} - c_R^{(k)}}{\alpha^{-1}\sigma_n}\right) \\ &- Q\left(\frac{-\tau - c_R^{(k)}}{\alpha^{-1}\sigma_n}\right) + Q\left(\frac{-\frac{\tau}{2} - c_R^{(k)}}{\alpha^{-1}\sigma_n}\right) \\ &- Q\left(\frac{-c_R^{(k)}}{\alpha^{-1}\sigma_n}\right) + Q\left(\frac{\frac{\tau}{2} - c_R^{(k)}}{\alpha^{-1}\sigma_n}\right) - Q\left(\frac{\tau - c_R^{(k)}}{\alpha^{-1}\sigma_n}\right) \\ &+ Q\left(\frac{\frac{3\tau}{2} - c_R^{(k)}}{\alpha^{-1}\sigma_n}\right) - Q\left(\frac{2\tau - c_R^{(k)}}{\alpha^{-1}\sigma_n}\right) \\ &+ Q\left(\frac{\frac{5\tau}{2} - c_R^{(k)}}{\alpha^{-1}\sigma_n}\right) - Q\left(\frac{3\tau - c_R^{(k)}}{\alpha^{-1}\sigma_n}\right), \end{aligned} \quad (25)$$

where  $c_R^{(k)} = \text{sgn}(\Re[x_k])\Re[\mathbf{h}_k^T \mathbf{d}]$ . Hence, the average BER of the in-phase component of  $\mathbf{y}$  is given by

$$P_{eI,\mathbf{x}}(\mathbf{d}) = \frac{1}{K} \sum_{k=1}^K P_{eI,k}(\mathbf{d}). \quad (26)$$

Similarly, let  $c_I^{(k)} = \text{sgn}(\Im[x_k])\Im[\mathbf{h}_k^T \mathbf{d}]$ . The BER of the quadrature-phase component for the  $k$ th user, denoted as  $P_{eQ,k}(\mathbf{d})$ , can be derived by replacing  $c_R^{(k)}$  with  $c_I^{(k)}$  in (25). Then the average BER for the quadrature-phase component of  $\mathbf{y}$  is given by

$$P_{eQ,\mathbf{x}}(\mathbf{d}) = \frac{1}{K} \sum_{k=1}^K P_{eQ,k}(\mathbf{d}). \quad (27)$$

The resultant average BER of  $\mathbf{y}$  is given by

$$P_{e,\mathbf{x}}(\mathbf{d}) = (P_{eI,\mathbf{x}}(\mathbf{d}) + P_{eQ,\mathbf{x}}(\mathbf{d}))/2. \quad (28)$$

Hence, the optimal effective symbol vector  $\mathbf{d}_{\text{opt}}$  is found by solving the following optimisation problem

$$\mathbf{d}_{\text{opt}} = \arg \min_{\mathbf{d}} P_{e,\mathbf{x}}(\mathbf{d}). \quad (29)$$

The problem (29) turns out to be a challenging non-convex optimisation with many local minima. As an illustration, Fig. 7 depicts the BER surface  $P_{e,x}(\mathbf{d})$  for the simplest case of  $N = 1$  and  $K = 1$ , with SNR = 16 dB. The PSO algorithm of Section 2 offers an efficient means to solve this optimisation problem, where the cost function is  $P_{e,x}(\mathbf{d})$  with the parameter vector  $\mathbf{d} \in \mathcal{U}^N$ . For the system given in Subsection 4.1, our empirical results suggested that  $U_{\max} = 1.2$  and  $V_{\max} = 0.2$  are appropriate. The inertia weight is chosen as  $\xi = rand()$ , which is seen to perform better in this application than the two alternative choices of  $\xi$ . In Step *a*), one of the initial particles is set to the improved MMSE-VP solution of (Yao et al., 2009a).

### 4.3 Simulation results

We consider the challenging MIMO system, where the BS employed  $N = 2$  transmit antennas to communicate with  $K = 4$  MSs. This system was rank deficient as the number of the BS transmit antennas was smaller than the number of MSs supported. Again, all the simulation results were obtained by averaging over 100 channel realisations. The received signals after the modulo operation were directly used for making decisions. Appropriate swarm size was found empirically to be  $S = 20$ , and the maximum number of iterations was ranging from  $I_{\max} = 20$  to 45 depending on the SNR value. Fig. 8 shows the BER performance of the linear MBER-MUT design presented in Section 3, the powerful nonlinear MMSE-VP design presented in (Schmidt et al., 2005), and the proposed PSO-aided MBER generalised VP design. The linear MBER MUT encountered a high error floor as it

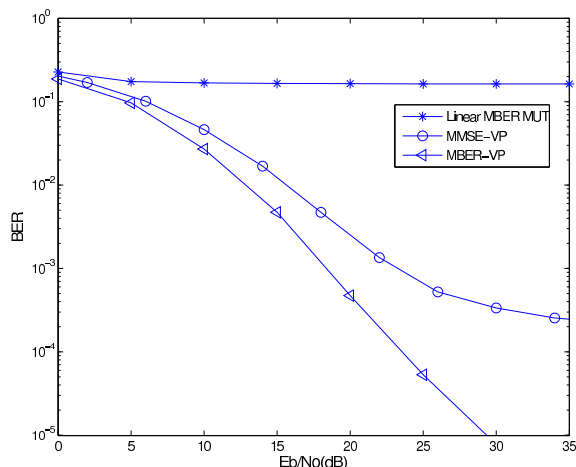


Figure 8: Performance comparison of the linear MBER-MUT, the nonlinear MMSE-VP and the proposed PSO-aided MBER generalised VP for the  $2 \times 4$  MIMO system.

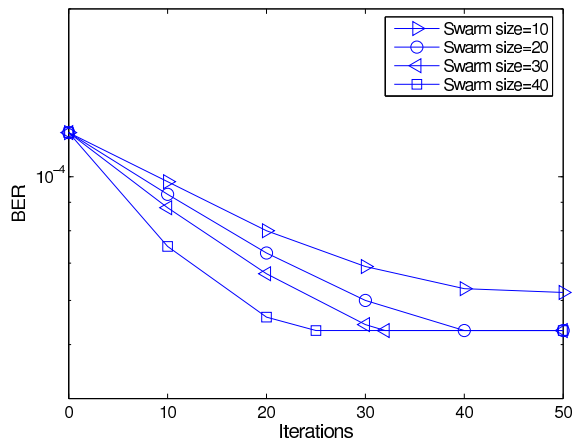


Figure 9: Convergence of the PSO-aided MBER generalised VP scheme with different swarm sizes for the  $2 \times 4$  MIMO system given SNR = 25 dB.

was unable to differentiate the users' information in this demanding scenario. The nonlinear MMSE VP scheme showed a much better performance but still suffered from an error floor as can be seen in Fig. 8. By contrast, the generalised MBER VP outperformed the MMSE VP and it did not exhibit a visible error floor which showed its ability to operate successfully in the rank-deficient scenario.

Fig. 9 shows that  $S = 10$  was insufficient for the PSO algorithm to attain the global optimal solution, while the PSO algorithm with  $S = 20, 30$  and  $40$  all converged to the optimal solution with  $I_{\max} = 40, 32$  and  $25$ , respectively. The computational complexity  $C_{\text{PSO}}$  for the PSO algorithm with  $S = 20, 30$  and  $40$  are compared in Table 3, which demonstrated that the choice of the swarm size  $S = 20$  for the PSO algorithm was optimal in terms of complexity in this case and explained why we used  $S = 20$  in the simulation. The computational complexity (Flops) as well as the recorded run times (s) of the two nonlinear MUT designs, namely the powerful MMSE-VP solution (Schmidt et al., 2005) and the proposed PSO-aided MBER generalised VP solution, are compared in Table 4, given the two SNR values. It can be seen from Table 4 that the complexity of the PSO aided MBER generalised VP design was no more than twice of the conventional MMSE-VP design. This was a

Table 3: Complexity (Flops) of the PSO aided MBER generalised VP design with different swarm sizes for the  $2 \times 4$  MIMO system, given SNR = 25 dB.

Swarm size $S$	Iterations $I_{\max}$	Complexity
20	40	4,064,937
30	32	4,149,627
40	25	4,174,077

Table 4: Complexity (Flops) and recorded run time (s) required by the MMSE-VP design and the PSO-aided MBER generalised VP design for the  $2 \times 4$  MIMO system given two SNR values.

(SNR= 25 dB)	MMSE-VP	MBER-VP
Complexity (Flops)	2,508,638	4,064,937
Run time (s)	4787.3	8878.9
(SNR= 30 dB)	MMSE-VP	MBER-VP
Complexity (Flops)	2,609,600	4,471,060
Run time (s)	4981.9	9565.8

small price worthy of paying, considering the significant performance enhancement of the former over the latter as shown in Fig. 8.

## 5 Conclusions

PSO has been invoked for designing optimal MUT schemes for MIMO communication systems. Our investigation has demonstrated that PSO aided designs are capable of attaining global or near global optimal solutions at affordable computational costs. More specifically, the PSO aided linear MBER MUT scheme has been shown to impose significantly lower computational complexity than the existing state-of-the-art SQP-based linear MBER MUT design, while a novel PSO aided nonlinear MBER generalised VP design has been demonstrated to outperform the powerful nonlinear MMSE VP solution at the cost of slightly increased complexity.

## REFERENCES

- Alias, M. Y., Chen, S., and Hanzo, L. (2005). Multiple antenna aided ofdm employing genetic algorithm assisted minimum bit error rate multiuser detection. *IEEE Trans. Vehicular Technology*, 54:1713–1721.
- Chen, S. and Wu, Y. (1998). Maximum likelihood joint channel and data estimation using genetic algorithms. *IEEE Trans. Signal Processing*, 46:1469–1473.
- Chen, S., Wu, Y., and McLaughlin, S. (1997). Genetic algorithm optimisation for blind channel identification with higher-order cumulant fitting. *IEEE Trans. Evolutionary Computation*, 1:259–266.
- Feng, H.-M. (2006). Self-generation rbfn using evolutionary pso learning. *Neurocomputing*, 70:241–251.
- Guru, S. M., Halgamuge, S. K., and Fernando, S. (2005). Particle swarm optimisers for cluster formation in wireless sensor networks. In *Proc. 2005 Int. Conf. Intelligent Sensors, Sensor Networks and Information Processing*, pages 319–324, Melbourne, Australia.
- Habendorf, R. and Fettweis, G. (2007). Nonlinear optimization for the multiuser downlink. In *Proc. 13th European Wireless Conf.*, page 7 pages, Paris, France.
- Hochwald, B. M., Peel, C. B., and Swindlehurst, A. L. (2005). A vector-perturbation technique for near-capacity multiantenna multiuser communication - part ii: perturbation. *IEEE Trans. Communications*, 53:537–544.
- Kennedy, J. and Eberhart, R. (1995). Particle swarm optimization. In *Proc. 1995 Int. Conf. Neural Networks*, volume 4, pages 1942–1948, Perth, Australia.
- Kennedy, J. and Eberhart, R. C. (2001). *Swarm Intelligence*. Morgan Kaufmann.
- Nocedal, J. and Wright, S. (1999). *Numerical Optimization*. Springer, New York.
- Ratnaweera, A., Halgamuge, S. K., and Watson, H. C. (2004). Self-organizing hierarchical particle swarm optimizer with time-varying acceleration coefficients. *IEEE Trans. Evolutionary Computation*, 8:240–255.
- Schmidt, D. A., Joham, M., and Utschick, W. (2005). Minimum mean square error vector precoding. In *Proc. PIMRC 2005*, volume 1, pages 107–111, Berlin, Germany.
- Soo, K. K., Siu, Y. M., Chan, W. S., Yang, L., and Chen, R. S. (2007). Particle-swarm-optimization-based multiuser detector for cdma communications. *IEEE Trans. Vehicular Technology*, 56:3006–3013.
- Vojčić, B. R. and Jang, W. M. (1998). Transmitter precoding in synchronous multiuser communications. *IEEE Trans. Communications*, 46:1346–1355.
- Xu, C., Hu, B., Yang, L.-L., and Hanzo, L. (2008a). Ant-colony-based multiuser detection for multi-functional antenna array assisted mc ds-cdma systems. *IEEE Trans. Vehicular Technology*, 57:658–663.
- Xu, C., Yang, L.-L., Maunder, R. G., and Hanzo, L. (2008b). Near-optimum soft-output ant-colony-optimization based multiuser detection for the ds-cdma. In *Proc. ICC 2008*, pages 795–799, Beijing, China.
- Yao, W., Chen, S., and Hanzo, L. (2009a). Improved mmse vector precoding based on the mber criterion. In *Proc. VTC2009-Spring*, page 5 pages, Barcelona, Spain.
- Yao, W., Chen, S., and Hanzo, L. (2010). Generalised vector precoding design based on mber criterion for multiuser transmission. In *VTC 2010-Spring*, Taipei, China, submitted.
- Yao, W., Chen, S., Tan, S., and Hanzo, L. (2009b). Minimum bit error rate multiuser transmission designs using particle swarm optimisation. *IEEE Trans. Wireless Communications*, 8:5012–5017.
- Yen, K. (2001). *Genetic Algorithm Assisted CDMA Multiuser Detection*. PhD thesis, School of Electronics and Computer Science, University of Southampton, Southampton, UK.